JOURNAL OF MATERIALS SCIENCE **36** (2001) 609–621

Fatigue damage and hysteresis in wood-epoxy laminates

C. L. HACKER*, M. P. ANSELL
Department of Engineering and Applied Science, University of Bath, Bath, BA2 7AY, UK

Wood-epoxy laminates were subjected to constant amplitude fatigue tests in tension-tension ($R = 0.1$), compression-compression ($R = 10$) and reverse loading ($R = -1$) in order to follow property changes and fatigue damage accumulation. Hysteresis loops were captured during these tests and the form of stress versus number of cycles to failure (*S*-*N*) curves was established. Reversed loading is the most damaging mode of cyclic stress application. In terms of static strengths, the wood laminate is weaker in compression than in tension. However at low levels of stress, following many fatigue cycles, the fatigue life is greater in compression-compression than in tension-tension. The shape of captured hysteresis loops is strongly influenced by loading mode. As subcritical damage develops, loop area increases and dynamic modulus falls. In reversed loading, loop bending and distortion is observed depending on whether the damage is tension- or compression-dominated or both. Maximum and minimum fatigue strains, the dynamic modulus and loop area have been plotted as a function of the number of fatigue cycles. The majority of damage occurs towards the end of the sample life but property changes can be detected throughout fatigue tests. Normalisation of fatigue data demonstrates that the fatigue behaviour of wood-epoxy laminates is consistent.

1. Introduction

Research into the response of wood to fatigue loads at the University of Bath [1] has been stimulated by the needs of the wind turbine blade industry in the UK. The Department of Trade and Industry, formerly the Department of Energy, funded three consecutive research programmes on wood fatigue which were administered by the Energy Technology Support Unit at Harwell. Strong industrial support was provided by Mark Hancock, currently Chief Engineer at Aerolaminates Ltd., Totton, Southampton, UK [2].

The African mahogany, *Khaya ivorensis*, was investigated in these research programmes because of its application in the production of commercial, wood composite, wind turbine blades. It is an inexpensive hardwood, available in the form of approximately 4 mm thick, rotary cut veneers, which enables turbine blades to be laid up rapidly in moulds. Furthermore, variations in the properties of veneers are relatively small as Khaya is sustainably grown in equatorial forests, which reduces variation in density due to the relatively small seasonal variations in climate. Khaya contains a high volume fraction of vessels, up to 1 mm in diameter, which during the lamination process allows the penetration of surplus resin into the wood structure, enabling the formation of coherent, thin glue lines.

Wood is well known to be stronger in tension than in compression [3] so fatigue life is also likely to depend on the mode of loading. As fatigue damage accumulates at cellular level under fixed amplitude load control, wood laminates become more compliant, resulting in changes in the amplitude of fatigue strains. Micro-scale damage in the cell wall [4] develops into macro-scale compression creases and cracks, increasing the compliance of the cellular structure. In tension-tension fatigue, both maximum and minimum cyclic strains are likely to increase positively. In compression-compression fatigue, maximum and minimum cyclic strains are likely to increase negatively. Reversed loading should logically result in a combination of these effects in the tension and compression parts of the cycle.

The dynamic modulus of elasticity is expected to fall in the course of a fatigue test in common with composite materials [5–8]. Energy dissipated per cycle should increase, manifested by an increase in the area of captured hysteresis loops, which represent stress plotted versus strain for individual fatigue cycles. In both tension-tension and compression-compression fatigue the mean stress is non-zero so creep should be observed. Where the mean stress is zero ($R = -1$) it might be supposed that there would be no creep. However creep may occur if the rate of creep damage development in the compressive and tensile parts of the reversed loading cycle is different. Creep development should coincide with changes in the slope of captured hysteresis loops, denoting a fall in the dynamic elastic modulus of

* *Present Address:* Ove Arup and Partners, Research and Development, 13 Fitzroy Street, London, W1P 6BQ, UK.

elasticity. The spectrum of fatigue responses described above directly influences the form of fatigue constant life diagrams for wood laminates [9] and controls life under variable amplitude loading [10].

The aim of this paper is to examine the response of laminated Khaya to fatigue in tension-tension, compression-compression and mixed mode tension-compression modes. Stress versus number of cycles to failure (S-N) characteristics are presented for these loading modes. Hysteresis loops, trapped throughout fatigue tests, are examined, allowing changes in dynamic modulus and energy dissipated per cycle to be monitored. A loop analysis programme (LPA), developed by nCode International Ltd., is used to process hystersis loop data in order to record changes in maximum and minimum strains, dynamic modulus and loop area as a function of number of fatigue cycles. These parameters reflect damage development in the Khaya laminates.

2. Experimental methods

2.1. Manufacture of wood laminates

Wood composite panels (approximately 600 mm by 900 mm) were laminated by the Wind Energy Group at their blade manufacturing plant in Southampton using the same materials and vacuum bagging technique used in blade production. The epoxy resin adhesive was applied with a roller to one side only of each veneer. Each sample comprised eight 4 mm thick, rotary cut Khaya veneer layers. Rotary cutting produces curved veneers, which are stored in flattened stacks. The veneer face is therefore a flattened, approximately tangential-longitudinal plane and the veneer edge is approximately a radial-longitudinal plane. The veneers were laminated with a structural-grade, two part, room temperature-curing, epoxy resin (Structural Polymer Systems Ampreg 20 system with cellulose micro-fibre and colloidal silica fillers). Four parts by weight of resin were thoroughly mixed with one part of hardener. The mixed resin was modified with 25% volume for volume microfibre filler and 25% volume for volume colloidal silica filler in order to control viscosity and wetting characteristics. All eight veneers were aligned with their longitudinal grain direction as closely parallel with the sample axis as possible. However it should be emphasised that there are natural variations in the grain orientation within each veneer. The stack of veneers was consolidated by vacuum bagging under a polyethlene sheet with an intermediate layer of polymer netting used as a release membrane. Air was removed from the vacuum bag with a rotary pump and the laminate was consolidated by atmospheric pressure as the adhesive cured.

2.2. Sample preparation

When the panels were fully cured they were cut into dumb-bell-shaped samples and ten samples were produced from each panel. Fig. 1 shows the sample geometry, which was developed by Bonfield and Ansell [2]. The samples were quite substantial, because in order to avoid splitting from the edges of the parallel gauge length into the curved zones between the gauge length and sample ends it was necessary for the curved zones to have a large radius of curvature. In addition, the samples had quite a high cross-sectional area (31 mm thick by 34 mm wide) in order to avoid buckling stability problems when loaded in compression.

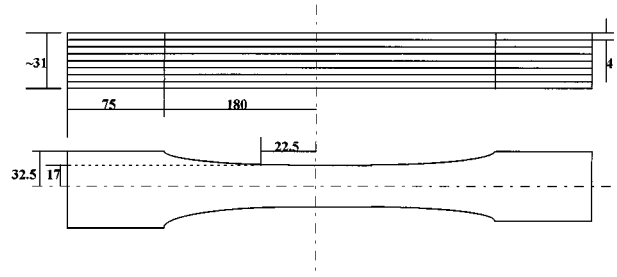

Figure 1 Sample geometry, dimensions in mm.

Samples were conditioned and tested at 65% relative humidity because the mechanical properties of wood are very sensitive to its moisture content [3]. Preconditioned samples for fatigue testing were enclosed in a sealed, polyethylene membrane constructed around the grips of the fatigue rig. This enclosure contained large beakers of saturated sodium nitrite solution which controlled the vapour pressure such that the air has a relative humidity of 65%. The laboratory temperature varied between 20 and 25°C.

2.3. Mechanical testing

Two, 20 tonne capacity, Mayes, servo-hydraulic fatigue machines were used for the fatigue evaluation of the wood composites. The servo-hydraulic grips were serrated and applied directly to the wood surface without the use of end tabs. The selection of grip pressure was critical in order to prevent either sample pull-out from the grips or fracture close to the grips away from the gauge length. The machines were equipped with Dartec model 9500 controllers which enabled stress versus strain hysteresis loops to be captured. For fatigue tests, a constant rate of stress application of 400 MPa·s^{-1} was selected, restricting the frequency of test to between 4 and 7 Hz. These frequencies are low enough to avoid sample heating, moisture loss and change in mechanical properties.

Two clip gauges were used to measure strains experienced by the wood composites. The gauge knife edges were located into small, grooved, steel tabs which were bonded to the gauge length of each sample using Araldite Rapid epoxy adhesive prior to each test. The steel tabs served to locate the clip gauges securely throughout a test and prevented the sharp blades damaging the sample surface and consequently initiating premature failure. The carefully calibrated gauges were clipped onto the sample using two steel springs and elastic bands at each end of the gauge.

Axial static tests were performed to determine ultimate tensile and compressive strengths. Ten samples were tested in tension and twelve in compression. The tests were controlled via the Dartec controller using a routine, which applied a single cycle in a triangular waveform at a rate of 10 MPa·s^{-1}. This is much slower than the rate used in fatigue tests (400 MPa·s^{-1})

and was adopted so that the samples did not pull out of the serrated grips and had sufficient time to bed in properly. A data capture file was written to accurately capture stress-strain information allowing the dynamic elastic modulus to be measured.

2.4. Hysteresis loop capture

Fatigue tests were run in the 'advanced capture' mode in order to collect stress-strain hysteresis loop data. A data capture file was written to capture loops at regular intervals throughout a test. A 'cycle trigger' was set to initiate data capture and at each trigger the Dartec controller recorded load and extension data until one loop of data had been recorded. The load data was derived from an output on the load cell and the extension data was collected via a clip gauge attached to the sample surface. Hysteresis loop capture was also triggered to great effect using the 'window trips' option. Once the test had been started a window was set around the maximum and minimum strain gauge outputs, for example 2.5% full scale deflection. As the test proceeded, creep and fatigue damage occurred and the strain values changed. The moment one value exceeded a trip value, hysteresis loop capture was triggered. The window then reset itself around the most recent trigger value. In this way data capture was triggered at points in the test where the strains were altering rapidly, particularly at the end of the test where it was easy to miss crucial property changes.

Fatigue analysis software supplied by nCode International Ltd. was used to process the stress versus strain hysteresis loops. A software package, LPA, was written to handle the loop analysis and enabled the Dartec data files containing raw data to be read, the scaling factors to be applied and the loop area ($J \cdot m^{-3}$), dynamic modulus (GPa), strains (dimensionless) and stresses (MPa) to be calculated for each loop. The data were imported into the spreadsheet package 'Quattro pro for Windows' where the data could be further manipulated and the properties expressed graphically.

Stress versus strain hysteresis loop data were captured for wood composites at three R ratios. The concept of the stress ratio R is explained in Fig. 2. Tests were performed in pure compression ($R = 10$), pure tension ($R = 0.1$) and reversed loading ($R = -1$) over a range of stress levels so that any stress-dependent differences in the fatigue response would become apparent. Between three and six tests were carried out at each R ratio/peak stress condition. These stress levels were chosen so that all the samples survived for between 10^2 and 10^7 cycles. A constant rate of stress application of 400 $MPa \cdot s^{-1}$ was used in all tests. Stress versus number of cycles to failure (S-N) curves were constructed from the tests at these three R ratios. A minimum of twenty hysteresis loops were captured during each decade of load cycling using the data capture facility. The capture rate increased considerably at the end of the test when properties changed rapidly as catastrophic damage occurred and the window trips were employed.

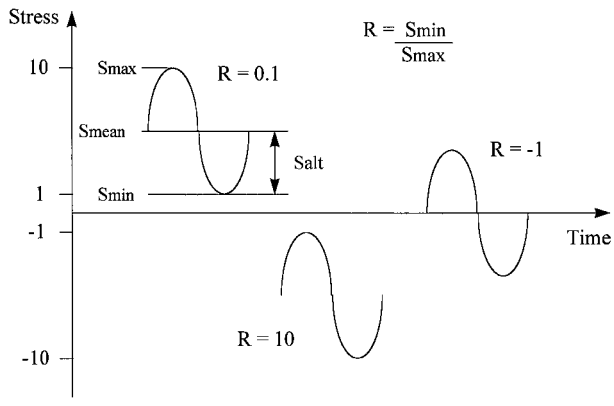

Figure 2 Definition of the stress ratio, R.

3. Experimental results and discussion

3.1. Tensile and compressive static strengths

A mean tensile strength of 85.41 MPa, with a standard deviation of ± 10.22 MPa, was measured from 10 tests, similar to the value obtained by Bonfield and Ansell [1] who reported a mean value of 81.8 ± 9.3 MPa. A mean value of the ultimate compressive stress (UCS) of 52.69 MPa, with a standard deviation of ± 4.86 MPa, was recorded from 12 tests. Bonfield and Ansell [1] tested 32 samples and obtained a mean value of 49.47 ± 2.77 MPa. A mean tensile tangent modulus of 9.43 GPa and a mean compressive tangent modulus of 10.06 GPa were calculated for tests reported here.

A typical compressive stress versus strain plot is presented in Fig. 3. The compressive stress increased linearly up to approximately 75% of the ultimate compressive strength and the maximum load was reached at a peak strain of -0.86%. At this point a macroscopic compression crease was formed which grew rapidly as the load was further applied. The load fell to zero at the point when the over-travel trip operated and stopped the test. The sample could still sustain a load even though it contained a compression crease, although the failed wood was weaker than in its undamaged state. However, once the crease had formed it made the wood unstable and the compression crease developed quickly. Dinwoodie [3] states that in compression the initial stages of damage appear microscopically at stresses as low as 25% UCS and that stress versus strain curves depart from linearity at between 30 to 50% of the failure

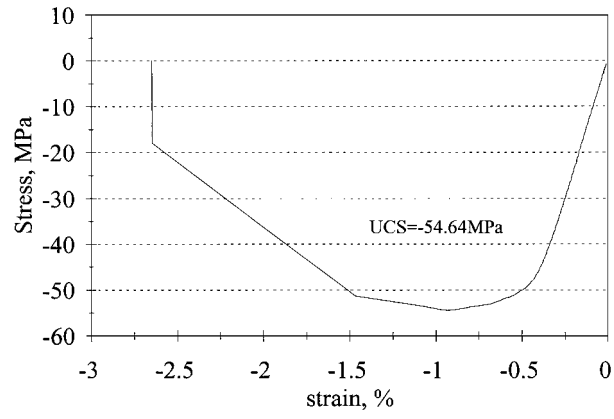

Figure 3 Static stress versus strain characteristic for typical Khaya specimen in compression.

stress. In these tests the wood laminates deformed linearly up to between 56% and 86% of the UCS. The mean strain to failure (taken as the point where the maximum load was sustained) for all tests was −1.03%, very close to the expected value of −1% [3].

3.2. *S-N* curves

S-log*N* data for fatigue tests at $R = 0.1$, $R = 10$ and $R = -1$ are presented in Fig. 4a–c. The static strengths are included at $\log_{10} N = -0.602$, when one quarter of a cycle has elapsed and the peak stress is reached. A line of best fit has been plotted through all the fatigue data points, but run-out samples (arrows) are excluded. The line of best fit is calculated statistically from *N*-*S* data, because *N* is the dependent variable. The data is then converted into the traditional *S*-*N* form. In tension-tension fatigue (Fig. 4a at $R = 0.1$) for lives of up to 10^7 cycles to failure, the data points all fall below the range of the ultimate tensile strength (UTS) data. The best linear fit line cuts the range of scatter in UTS values but falls below the scatter of run out values. Jagged failure occurred in the necked portion of the sample with some failure occurring close to, but not at, the glued interfaces in the tangential-longitudinal plane.

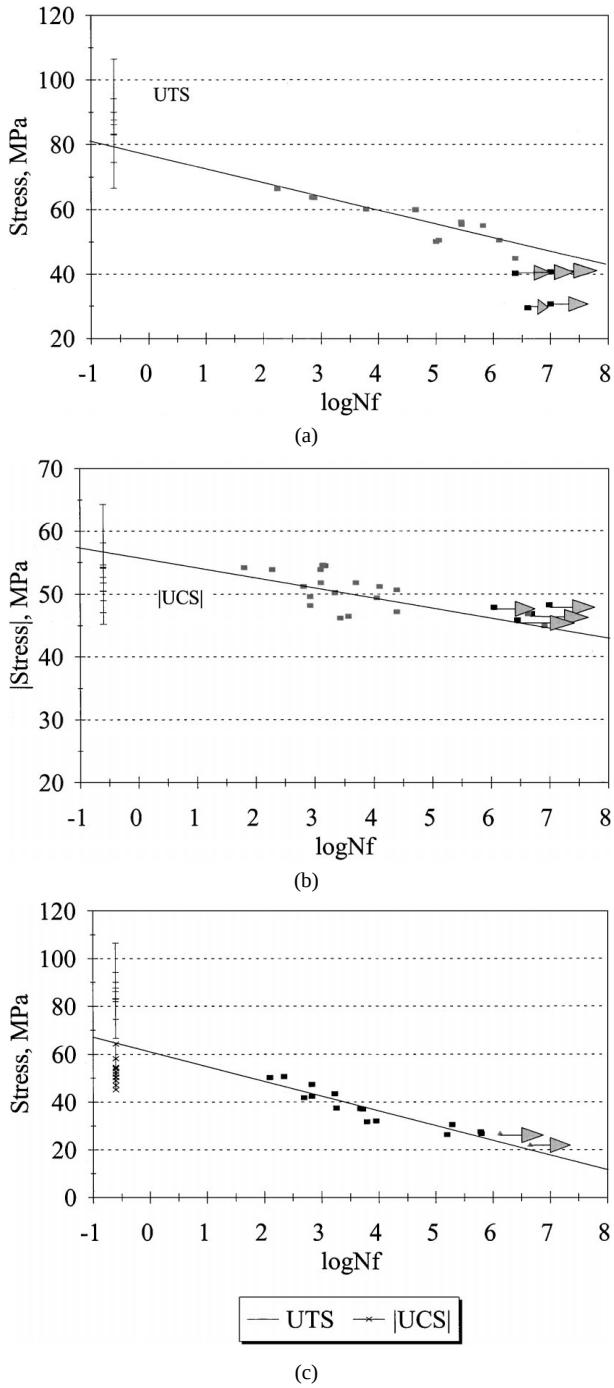

Figure 4 Stress versus log cycles to failure plots for Khaya in (a) tension-tension fatigue at $R = 0.1$, (b) compression-compression fatigue at $R = 10$ and (c) reversed loading fatigue at $R = -1$.

In compression-compression fatigue (Fig. 4b at $R = 10$) the data points fit between a small window of peak stresses and the numerical modulus of stress is plotted. The curve of linear fit passes through the range of UCS data and has a much lower slope than at $R = 0.1$. The curve also intersects the cluster of run out points. It is clear that, expressed as a percentage of mean UCS and mean UTS, wood is more fatigue tolerant in compression-compression than it is in tension-tension. Indeed at a peak stress of 40 MPa samples loaded at $R = 10$ can expect to survive more cycles of stress than samples loaded at $R = 0.1$. Failure in compression-compression manifested itself in the form of macroscopic compression creases which ran diagonally across the tangential longitudinal face (flat face of veneers) of the sample. On the radial-longitudinal face (veneer layers and glue lines visible), unevenly ruptured veneers were observed at the end of the macroscopic crease.

In reversed loading fatigue (Fig. 4c at $R = -1$) the line of best fit through the fatigue points falls between the two clusters of static strength data points for UTS and UCS at $\log_{10} N = -0.602$ and also lies close to the two run out points. The range of stress levels over which failure occurred for lives of up to 10^7 cycles is the highest for the three *R* ratios under consideration and consequently the line of best fit has the highest gradient. Hence reversed loading is the most damaging mode of testing for Khaya laminate in fatigue because damage caused in the compressive half of the cycle is opened up in the tensile part of the cycle. This trend in behaviour was reported in four-point bending by Tsai and Ansell [4]. The mode of failure essentially combines the features of tensile and compressive failure with some compressive shear and some longitudinal cracking.

It is informative to compare the fall in fatigue strength for each *R* ratio per decade of cycles by comparing the slopes of Fig. 4a–c. At $R = 0.1$ (tension-tension) the fatigue strength falls by 4.4% per decade of life in cycles, normalised by the mean UTS. At $R = 10$ (compression-compression) the fatigue strength falls by 2.8% per decade of life, normalised by the mean UTS. At $R = -1$ (reversed loading) the fatigue strength falls by 11.8% per decade of life, normalised by the mean UCS and 7.3% per decade of life, normalised by the mean UTS. The damaging effect of the three fatigue modes is investigated in Section 3.3.

3.3. Hysteresis loop capture at $R = 10$

Changes in the mechanical properties of wood composites as a result of fatigue damage are reflected in the

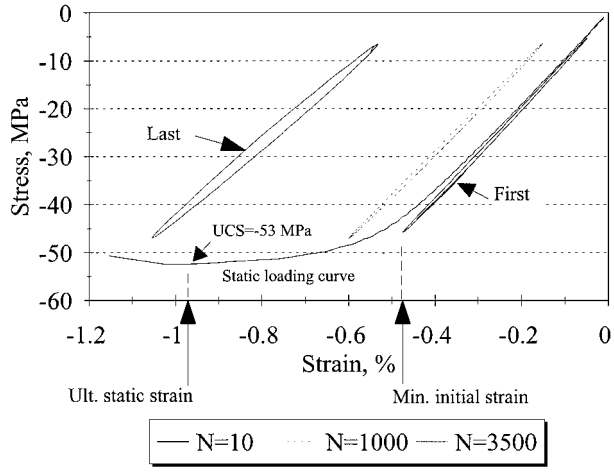

Figure 5 Stress plotted versus strain for Khaya in compression at a minimum stress of −47.5 MPa at $R = 10$. One static curve and three captured hysteresis loops at $N = 10$, 1,000 and 3,500 cycles are included.

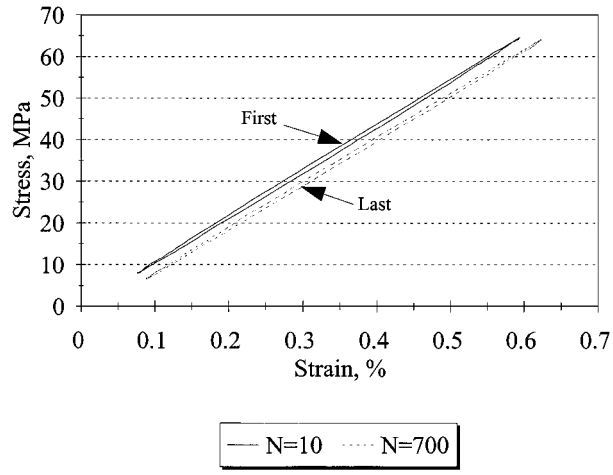

Figure 6 First and last captured hysteresis loops for Khaya in tension-tension fatigue at $R = 0.1$ and a peak stress of 65 MPa.

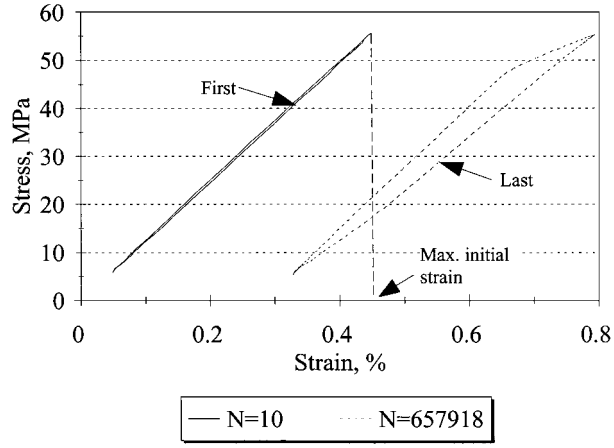

Figure 7 First and last captured hysteresis loops for Khaya in tension-tension fatigue at $R = 0.1$ and a peak stress of 55 MPa.

changes in shape of hysteresis loops captured throughout a test. The area within a hysteresis loop is the energy dissipated per cycle ($J \cdot m^{-3}$) and the average slope of the loop (maximum peak to minimum peak) is the dynamic modulus. A series of stress versus strain hysteresis loops captured during a compression fatigue test at $R = 10$ is presented in Fig. 5. A static loading curve from a different sample is included for comparison. The slope of first hysteresis loop approximately follows the static loading curve. As fatigue proceeds compressive creep occurs under the action of the compressive fatigue load and the hysteresis loops move along the negative strain axis. The last loop captured before failure has a minimum strain of −1.05%, close to the static strain to failure. The last loop is also less steep and broader than the first loop. This is indicative of the accumulation of fatigue damage in the composite.

It can be appreciated that the minimum stress in the fatigue test is extremely close to the mean static UCS (53 MPa) of the wood composite. In order to observe the development of fatigue damage in compression-compression it is necessary to test at such high compressive stress levels because the *S-N* curve is very shallow (Fig. 4b). At stress levels 20% below the mean static UCS, failure would not have occurred within a run-out limit of 10^7 cycles. When testing so close to the mean UCS it is not surprising that there is considerable scatter in fatigue lifetimes because the minimum stress is within the range of variation in UCS.

3.4. Hysteresis loop capture at $R = 0.1$

The first and last hysteresis loops captured in tension-tension fatigue tests at $R = 0.1$ are presented in Figs 6 and 7. In the first case the peak stress of 65 MPa (Fig. 6), equivalent to 76% of the mean static strength, results in a short fatigue life and the last captured loop is shifted slightly along the positive strain axis and the loop area appears almost identical. Fatigue failure is fracture-dominated and very little volume damage is apparent. At a peak stress of 55 MPa (Fig. 7), equivalent to 64% of the mean static strength, fatigue life is much longer, extensive tensile creep has occurred, there is a decrease in dynamic modulus and the loop area has clearly increased. There is also some distortion in the hysteresis loop demonstrating that the dynamic response of the wood laminate on loading is different to the response on unloading.

All the samples tested at the lowest peak stress levels of the order of 30 to 40 MPa were run outs (had not failed at 10^7 cycles) and suffered negligible fatigue damage because they were stressed below the elastic limit. At intermediate stress levels, close to or above the elastic limit, where pronounced changes in loop shape were observed, longitudinal cracks were seen to build up in the composite as fatigue proceeded. At high stress levels failure occurred without any dramatic changes in properties. A gradual build-up of cracks was not evident and failure was instantaneous. It is likely that, at the high stress levels, once a crack in a veneer is formed it leads to immediate failure; but at lower stress levels the cracks are not critical and grow gradually, causing a decrease in modulus and increase in loop area until failure.

3.5. Hysteresis loop capture at $R = -1$

Changes in dynamic properties under reverse loading are, not surprisingly, the most complex of the three loading configurations, as they are determined by

cumulative fatigue damage of the wood composite in both tension and compression. Three different types of fatigue response were identified, namely compression-dominated (Fig. 8), tension-dominated (Fig. 9) and a combination of the two responses (Fig. 10). The fatigue response at $R = -1$ is related to the mode of failure initiation rather than to the level of peak stress.

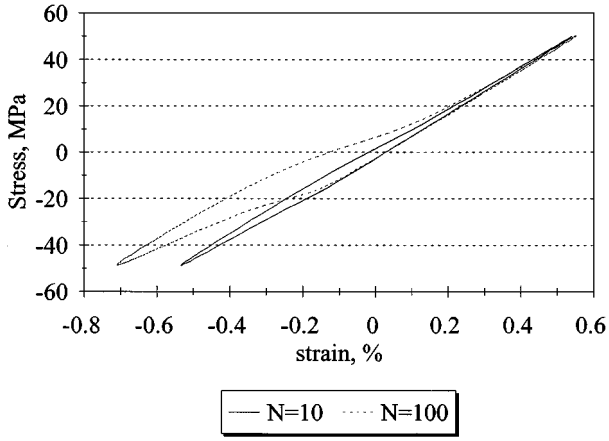

Figure 8 Captured hysteresis loops for Khaya in reversed loading at $R = -1$ and a peak stress of ± 50 MPa after 10 and 100 cycles. Loop shape is compression-dominated.

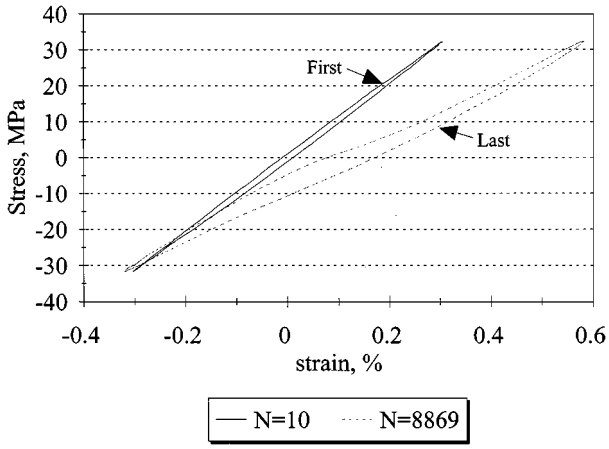

Figure 9 Captured hysteresis loops for Khaya in reversed loading at $R = -1$ and a peak stress of ± 32 MPa after 10 and 8,869 cycles. Loop shape is tension-dominated.

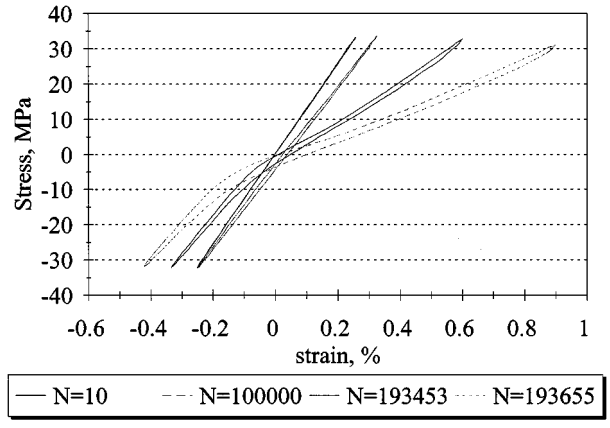

Figure 10 Captured hysteresis loops for Khaya in reversed loading at $R = -1$ and a peak stress of ± 35 MPa after 10, 100,000, 193,453 and 193,655 cycles. Loop shape is influenced by tension- and compression-generated damage.

In compression-dominated fatigue (Fig. 8) the maximum tensile strain remained unchanged but the minimum compressive strain decreased considerably. In tension-dominated fatigue (Fig. 9) the peak tensile strain increased considerably whilst the compressive minimum hardly changed at all. In each case, the dynamic modulus decreased with time and the loop area increased with some distortion according to the deformation mode. Both of these responses are merged in the combined response (Fig. 10) where both the maximum tensile and minimum compressive strains have changed considerably. The maximum tensile strain for the last loop captured after 193,655 cycles is very close to the expected ultimate static tensile strain of wood (1%). The increase in the negative compressive strains is less marked and the result is that the hysteresis loop bends and the tensile and compressive moduli are different from each other. Some samples only showed minor changes in loop shape and were judged to have exhibited an intermediate response.

Fractured samples for each response type were inspected. They showed distinct differences in failure mode. Samples with hysteresis loops, which exhibited large degrees of loop bending before failure, contained many longitudinal cracks, in radial-longitudinal planes. This was particularly noticeable where the outer veneers were at a shallow angle to the axis of the sample. Samples failing without loop bending contained more evidence of compression damage in the form of compression creases on the sample surfaces and the lifting of the grain to form splinters, which is a characteristic of tension fatigue damage, was much reduced.

3.6. Property changes in fatigue at $R = 10$

In compression-compression fatigue at a peak (negative) stress of -52.5 MPa the maximum and minimum strains decrease by similar amounts and compressive creep is significant (Fig. 11). This observation is to be expected, as the peak fatigue stress is close to the ultimate static compressive strength of the composite. Three of the five test samples (a, b and c) included in Fig. 11 follow a trend whereby the smallest increase in creep strain (negative) is related to the longest fatigue life. However, samples d and f do not conform to this trend.

The dynamic moduli for these samples vary between 9.4 and 11.8 GPa at the beginning of the fatigue tests. In all cases, except for sample d, a significant fall in modulus had occurred at the point of failure. The value of the dynamic modulus and the severity of the rate of fall in modulus depends on the precise orientation of veneers which make up the wood composite specimens. Likewise, rate of change in loop area (Fig. 13) is variable, but there is a general upward trend.

3.7. Property changes in fatigue at $R = 0.1$

At $R = 0.1$ (Fig. 14) the maximum and minimum fatigue strains are monitored for a peak tensile stress of 55 MPa. Initially there is only a small positive increase in these quantities but close to failure there is a marked increase in strain. Maximum strain changes much more

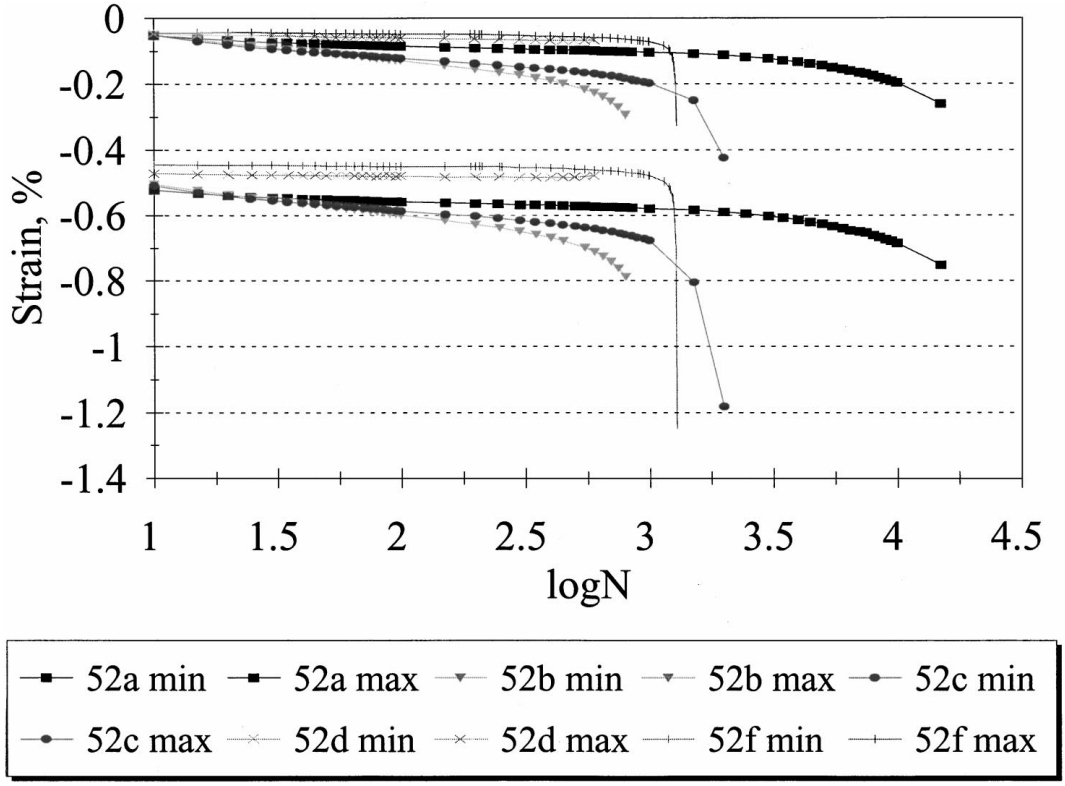

Figure 11 Maximum and minimum strain plotted versus log cycles for five Khaya specimens in compression fatigue at $R = 10$ and a minimum stress of -52.5 MPa.

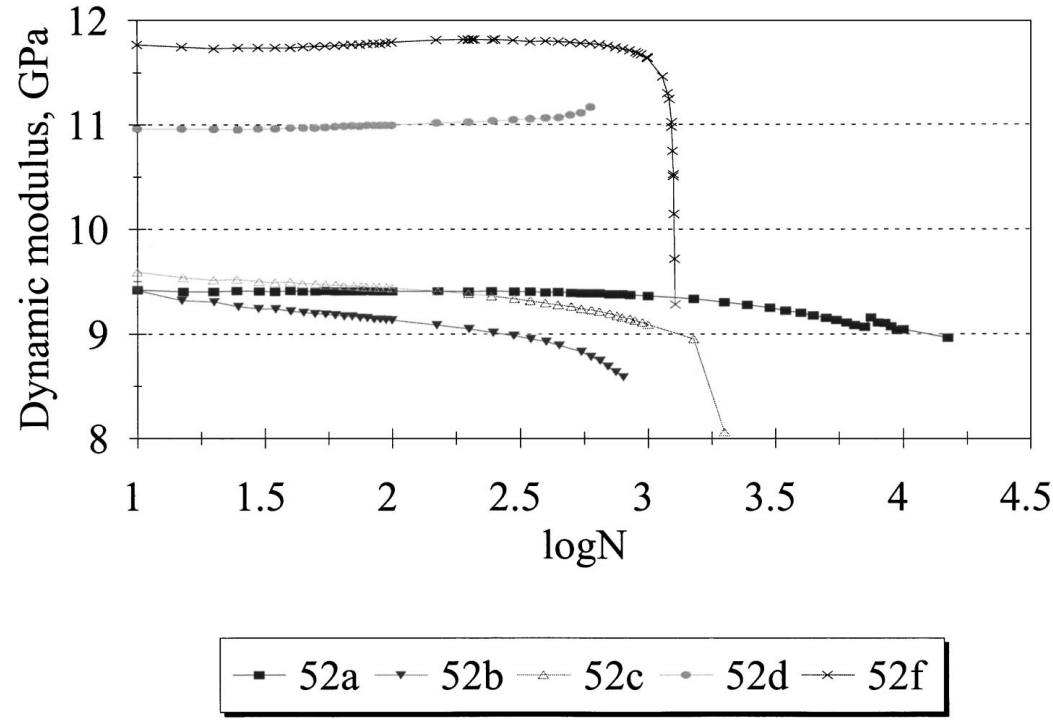

Figure 12 Dynamic modulus plotted versus log cycles for five Khaya specimens in compression fatigue at $R = 10$ and a minimum stress of -52.5 MPa.

significantly than the minimum strain in samples b, d and e. This is commensurate with a fall in the slope of the hysteresis loop which is confirmed by Fig. 15 which presents the dynamic modulus plotted versus log cycles. In tension-tension the loop area, Fig. 16, changes little until the end of the test, although it should be noted that results are plotted on a log scale.

Property changes in tension-tension fatigue are irregular due to the initiation and growth of fatigue cracks along the wood grain causing less consistent increases in the strains seen by the sample. Crack initiation causes small step increase in strain (Fig. 14). At the end of the test small, intermittent changes in properties (Figs 14–16) are likely to be due to the slight lifting

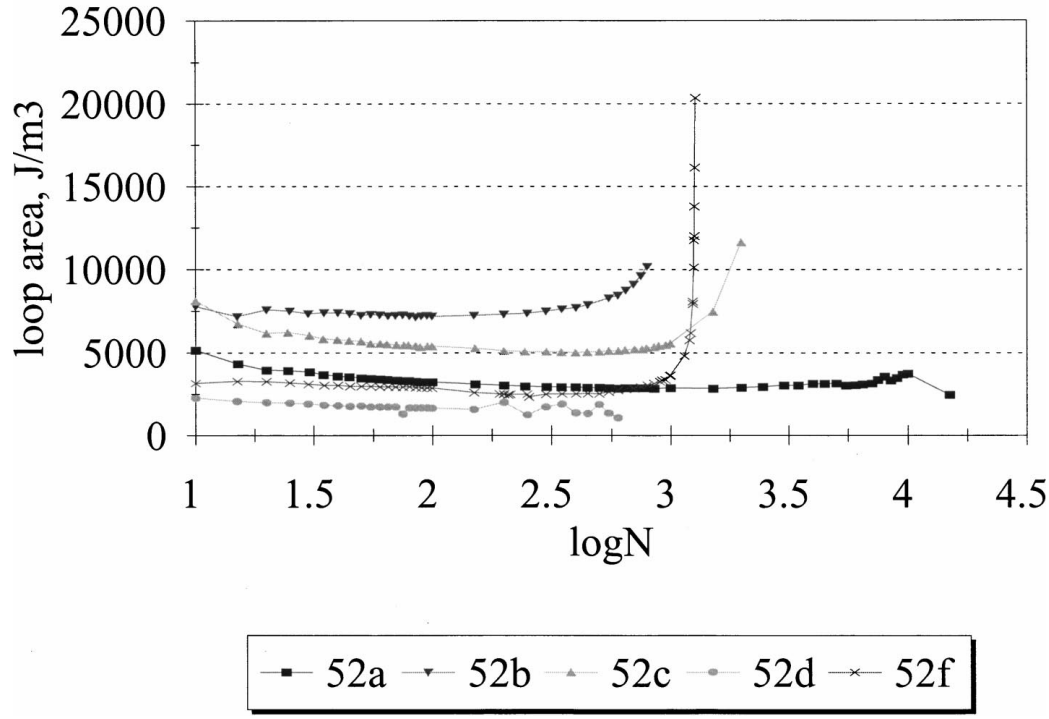

Figure 13 Hysteresis loop area plotted versus log cycles for five Khaya specimens in compression fatigue at $R = 10$ and a minimum stress of −52.5 MPa.

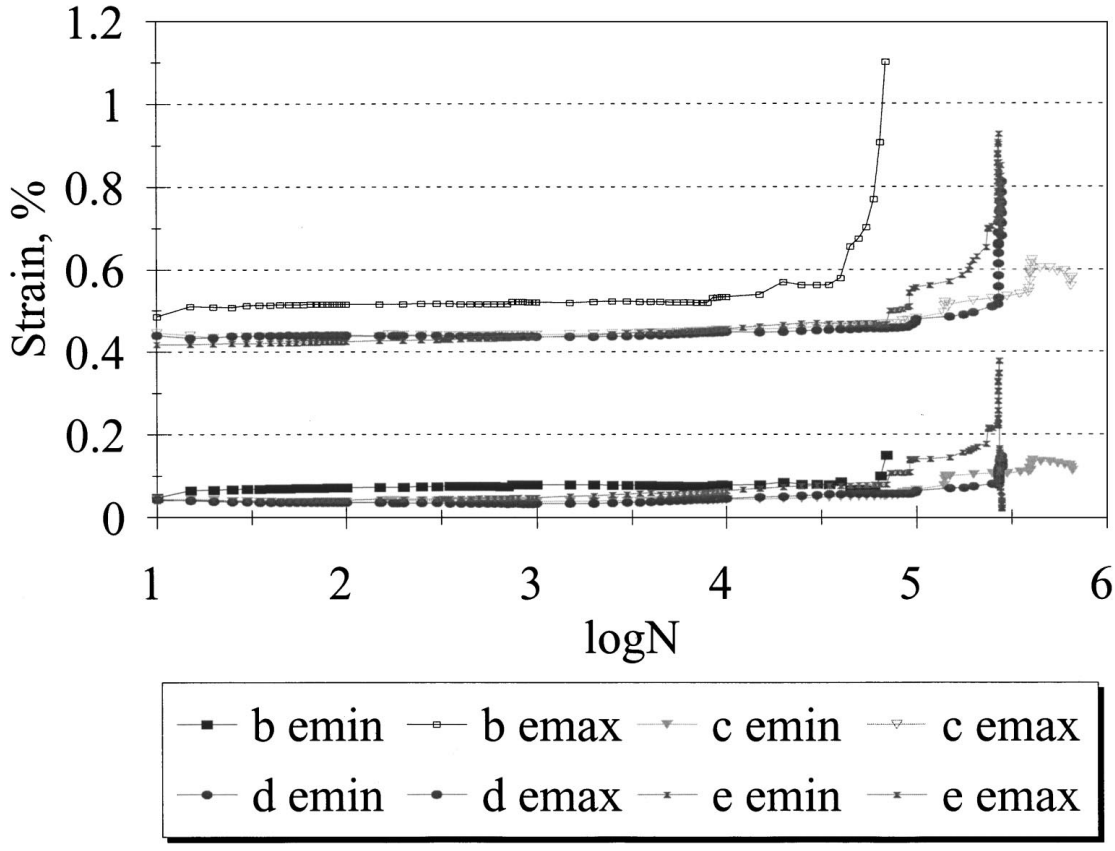

Figure 14 Maximum and minimum strain plotted versus log cycles for four Khaya specimens stressed in tension-tension fatigue at $R = 0.1$ and a peak stress of 55 MPa.

of the clip gauge from the sample surface as the cracked wood is cyclically loaded.

3.8. Property changes in fatigue at $R = -1$

The fatigue response in reversed loading is intriguing in the sense that property changes are better defined. The relationship between maximum and minimum strains (Fig. 17) for a peak stress of ±35 MPa is broadly symmetrical when plotted versus log cycles. However, the maximum strain always increases by more than the decrease in minimum strain, which is reflected by the bending of hysteresis loops (eg. Fig. 10). There is a

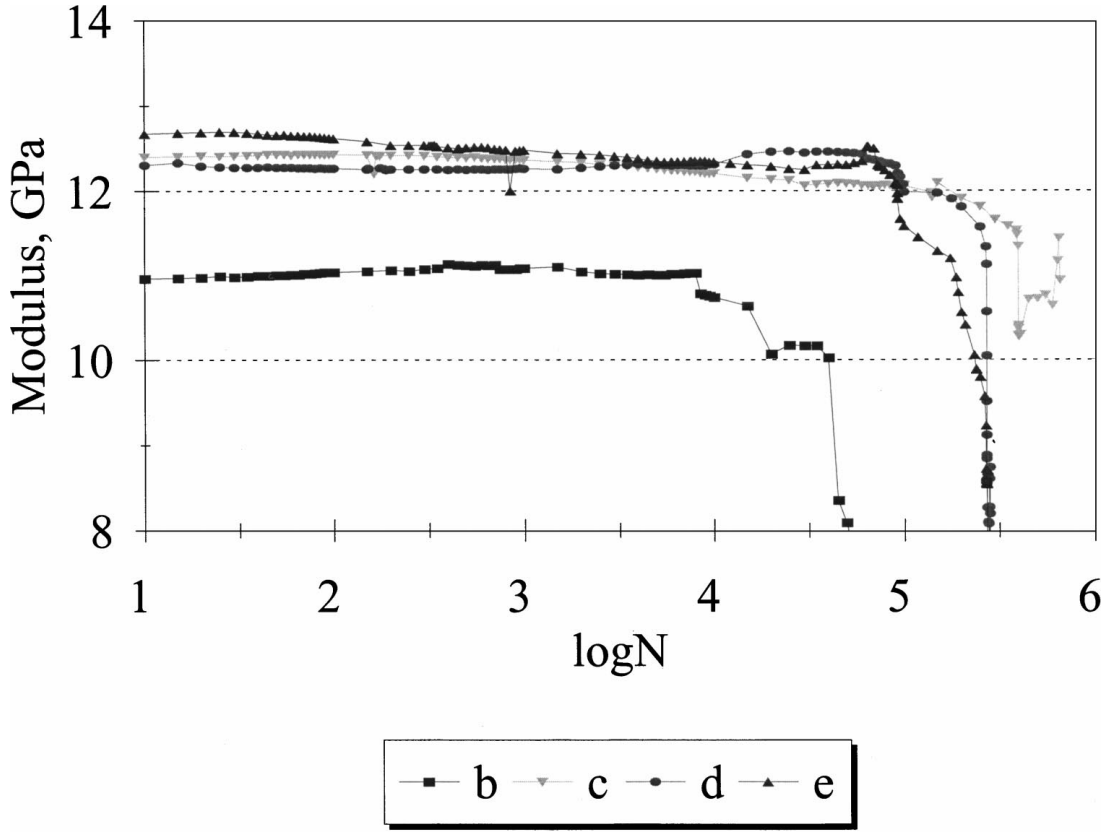

Figure 15 Dynamic modulus plotted versus log cycles for four Khaya specimens stressed in tension-tension fatigue at $R = 0.1$ and a peak stress of 55 MPa.

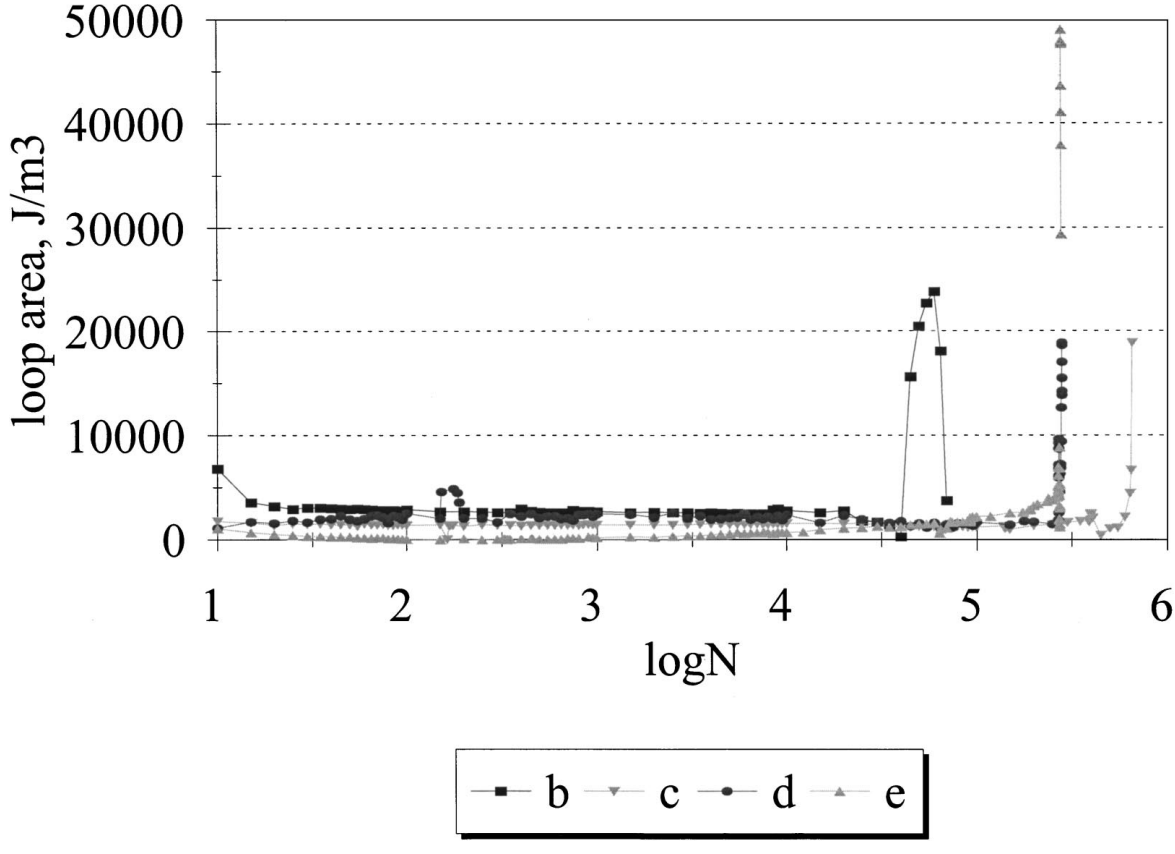

Figure 16 Hysteresis loop area plotted versus log cycles for four Khaya specimens stressed in tension-tension fatique at $R = 0.1$ and a peak stress of 55 MPa.

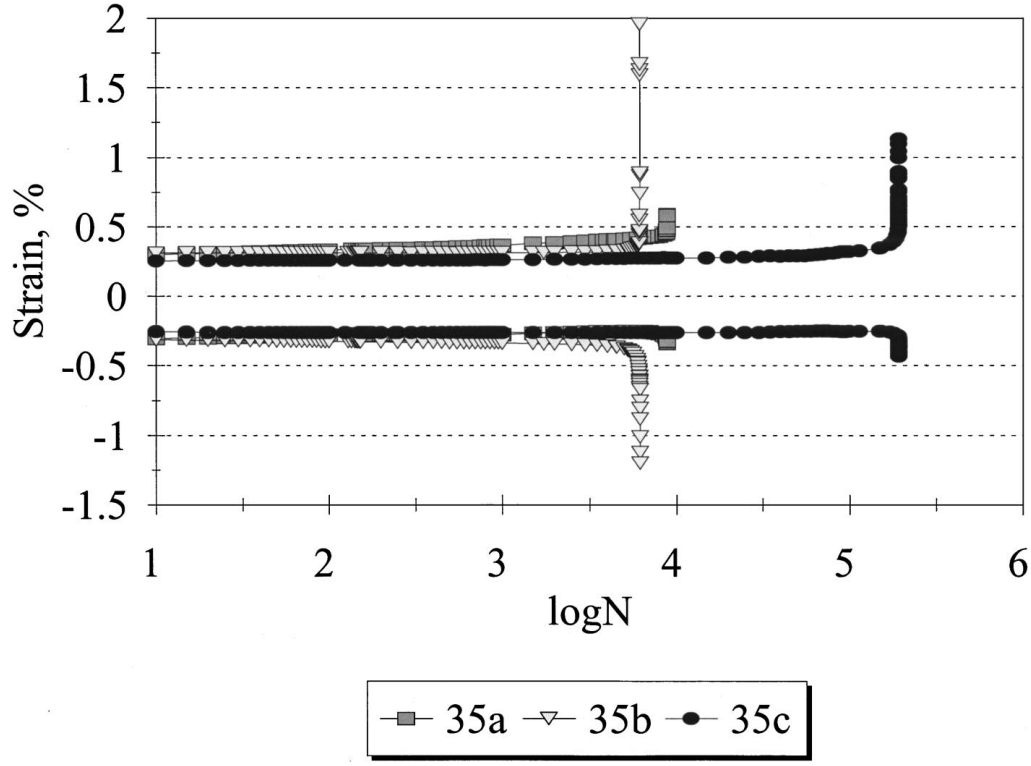

Figure 17 Maximum and minimum strain plotted versus log cycles for three Khaya specimens stressed in reversed loading at $R = -1$ and a peak stress of ± 35 MPa.

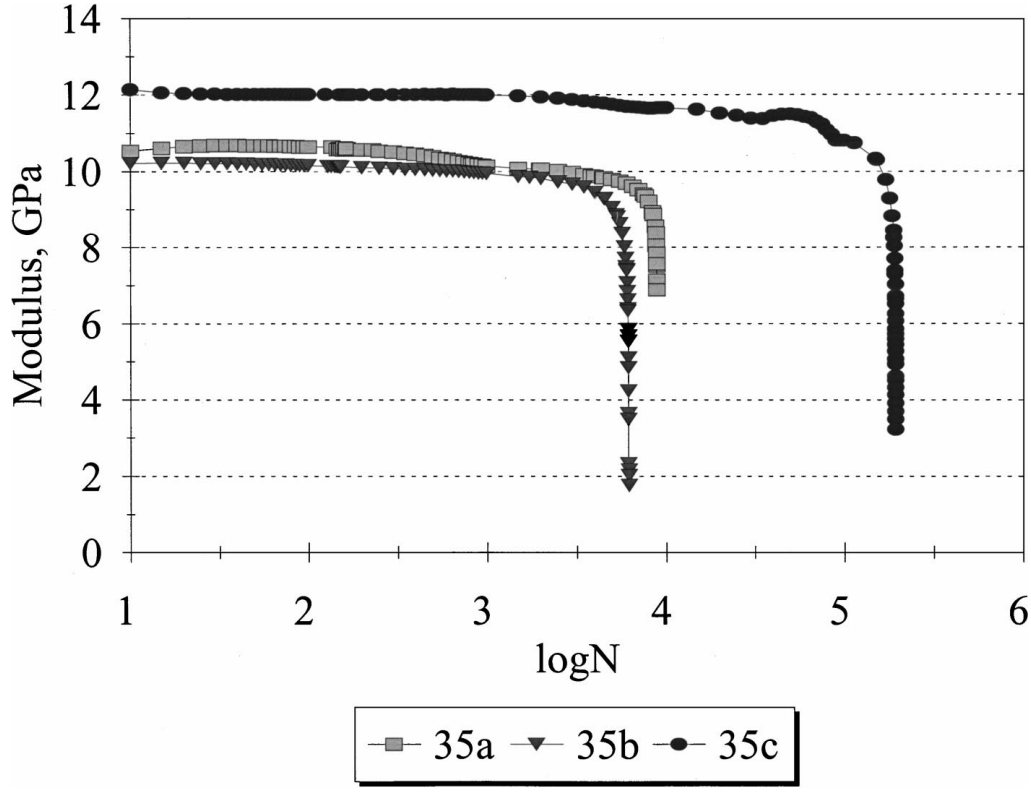

Figure 18 Dynamic modulus plotted versus log cycles for three Khaya specimens stressed in reversed loading at $R = -1$ and a peak stress of ± 35 MPa.

more progressive decline in dynamic modulus, Fig. 18. One sample, (b), experiences a degradation in dynamic modulus to less than 20% of its initial value. The most marked changes in dynamic modulus are observed in this reverse loading case. Loop area increases rapidly, Fig. 19, just before the onset of failure.

3.9. Normalised property changes at $R = -1$

An informative way of presenting dynamic modulus (Fig. 18) and loop area (Fig. 19) data in reversed loading is to normalise the x- and y-axes. In Fig. 20 the dynamic modulus (mod) is divided by its initial value (mod0) and the number of cycles (N) is divided by the total

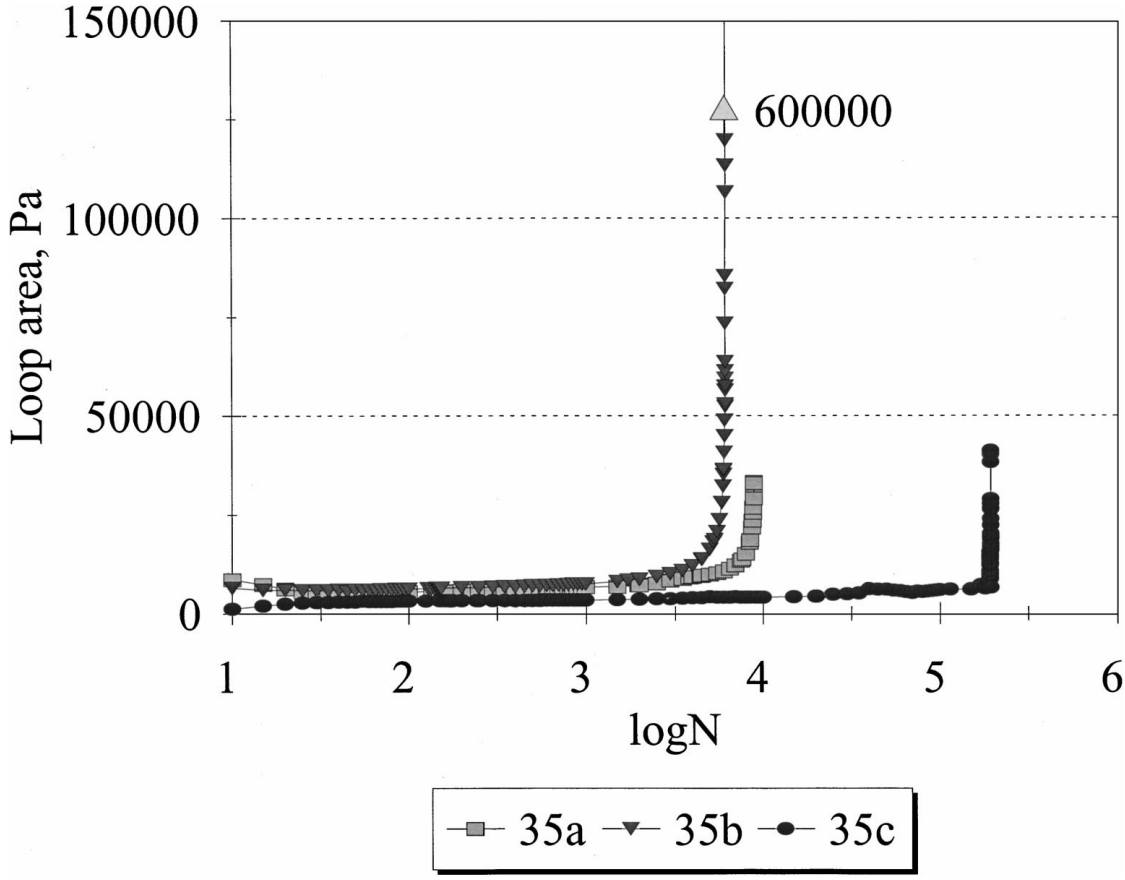

Figure 19 Hysteresis loop area plotted versus log cycles for three Khaya specimens stressed in reversed loading at $R = -1$ and a peak stress of ± 35 MPa.

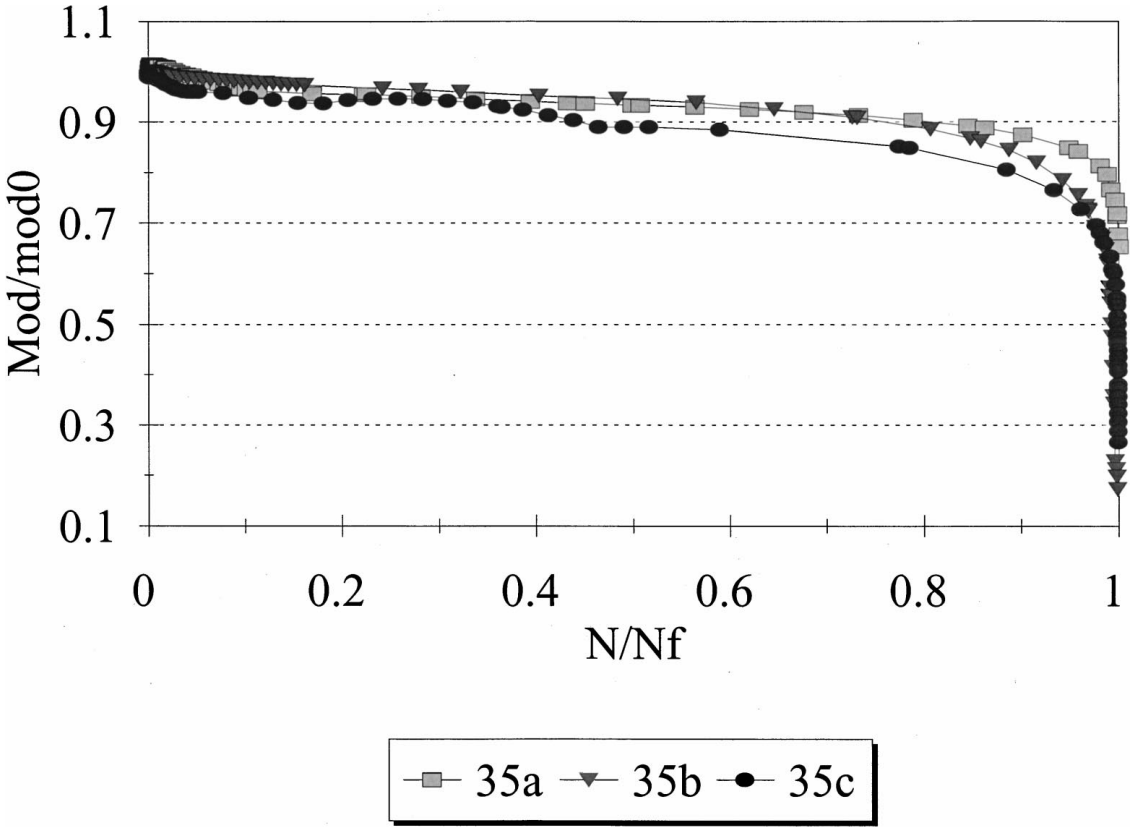

Figure 20 Normalised dynamic modulus plotted versus normalised cycles for three Khaya specimens stressed in reversed loading at $R = -1$ and a peak stress of ± 35 MPa.

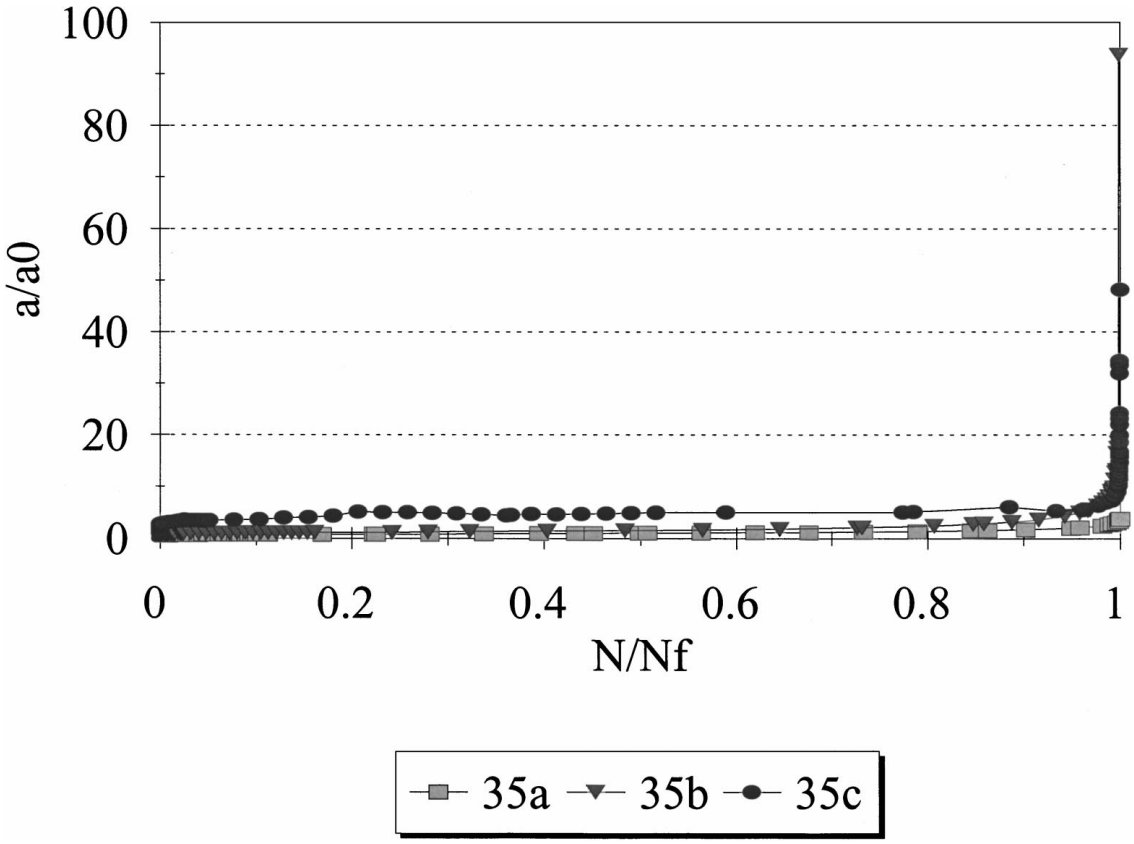

Figure 21 Normalised hysteresis loop area plotted versus normalised cycles for three Khaya specimens stressed in reversed loading at $R = -1$ and a peak stress of ± 35 MPa.

number of cycles to failure (Nf). The steady decline in dynamic modulus is consistent and clear. Normalised hysteresis loop area is plotted versus normalised cycles in Fig. 21 and again the underlying trend in property change becomes apparent and reproducible. This approach minimises the inherent variability between samples associated with inevitable natural differences in their micro- and macro-structure and the orientation of each wood veneer.

3.10. Damage under design loads

Wood and wood laminates are highly effective in preventing the propagation of cracks across the grain. Accordingly, damage accumulation in fatigue is not restricted to plane surfaces, as in metals, but it is a widespread, notch-insensitive, bulk process. When usual design safety factors are imposed on wood laminates they become highly fatigue tolerant.

4. Conclusions

- Stress versus strain hysteresis loop capture has been used successfully to follow fatigue damage accumulation in wood composites in compression-compression, tension-tension and reversed loading fatigue. Different fatigue responses have been observed in each loading mode.
  - In compression-compression at $R = 10$ the minimum stress level must lie within the scatter band of the ultimate static strength of the composite if fatigue failure is to occur. This is a result of the excellent fatigue performance of wood in compression and as a result the fatigue response of any individual sample will be linked to the ultimate compressive strength of that particular sample.
  - In tension-tension at $R = 0.1$ changes in loop shape and area were generally small for run-out samples where negligible fatigue damage occurred and at high stress levels where failure was almost instantaneous. At intermediate stress levels, where progressive crack growth along the grain was observed in the wood composite, changes in tensile creep, loop area and dynamic modulus were pronounced.
  - In reversed loading at $R = -1$ three distinct modes of fatigue damage accumulation were observed, namely compression-dominated, tension-dominated and both compression-and tension-dominated. Compression dominated damage occurred at high stress levels where the minimum stress was close to the mean UCS. Tension-dominated and mixed mode damage development occurred at lower stress levels.
  - In general the fatigue strain increases in the direction of the applied stress but significant changes in strain occur at the end of a sample's fatigue life. The dynamic modulus decreases and the loop area increases for all three R ratios. However the loop area may decrease marginally at the start of a test before increasing rapidly at failure.
  - Wood laminates are highly fatigue-tolerant at normal design stress levels, in applications such as wind turbine blades, where negligible fatigue damage will occur.

Acknowledgements

The authors are grateful to the Energy Technology Support Unit (Department of Trade and Industry) for funding Contract No. W/44/00287 and to the Engineering and Physical Sciences Research Council for funding a CASE award which supported this research. Mark Hancock provided generous industrial support during his time with Gifford and Partners, Gifford Technology Ltd., Composite Technology Ltd., the Wind Energy Group, Taywood Aerolaminates and in his current post as Chief Engineer at Aerolaminates Ltd.

References

1. M. P. ANSELL, M. HANCOCK and P. W. BONFIELD, in Proceedings of the 1991 International Timber Engineering Conference, London (TRADA, 1991) Vol. 4, p. 194.
2. P. W. BONFIELD and M. P. ANSELL, *J. Mat. Sci.* **26** (1991) 4765.
3. J. M. DINWOODIE, "Timber its Nature and Behaviour" (Van Nostrand Reinhold Co. Ltd., Workingham, UK, 1981).
4. K. T. TSAI and M. P. ANSELL, *J. Mat. Sci.* **22** (1990) 865.
5. J. N. YANG L. J. LEE and D. Y. SHEU, *Composite Structures* **21** (1992) 91.
6. L. YE, *Composite Science and Technology* **36** (1989) 339.
7. J. A. M. FERREIRA, J. D. M. COSTA, P. N. B. REIS and M. O. W. RICHARDSON, *Comp. Sci. and Tech.* **59** (1999) 1461.
8. W. B. HWANG and K. S. HAN, in "Composite Materials: Fatigue and Fracture," Vol. 2, edited by P. A. Lagace (ASTM, Philadelphia, 1989) p. 87, ASTM STP102.
9. I. P. BOND and M. P. ANSELL, *J. Mat. Sci.* **33** (1998) 2751.
10. *Idem., ibid.* **33** (1998) 4121.

Received 1 December 1999
and accepted 12 July 2000